Journal of Applied Fluid Mechanics, Vol. 10, No. 6, pp. 1649-1655, 2017.
Available online at www.jafmonline.net, ISSN 1735-3572, EISSN 1735-3645.
DOI: 10.29252/jafm.73.245.27148

Characteristics of CNG Bubbles in Diesel Flow under the Influence of the Magnetic Field

H. A. Abdul Wahhab[1], A. R. A. Aziz[1†], H. H. Al-Kayiem[2] and M. S. Nasif[2]

[1]*Centre for Automotive Research and Electric Mobility, Mechanical Engineering Department, Universiti Teknologi PETRONAS, Seri Iskandar, Perak, 32610, Malaysia*
[2]*Mechanical Engineering Department, Universiti Teknologi PETRONAS, Srei Iskandar, Perak, 32610, Malaysia*

†*Corresponding Author Email:* Rashid@utp.edu.my

(Received September 3, 2016; accepted September 7, 2017)

ABSTRACT

This paper conducts an analytic study of the hydrodynamics of a small CNG bubbles in laminar horizontal Diesel flow under the influence of the magnetic field. Investigation based on experiments was carried out to identify the effects caused by varying the magnetic field intensity on the trajectory, the formation of bubbles and their shape and velocity. Different images at different positions were captured through a high speed camera, image processing technique and downstream from the CNG bubbles injection point delivered information on bubble velocity, bubbles size, spatial location and gas area fraction as a function of changing magnetic field intensity. The outcomes confirmed that CNG bubbles under magnetic field grow up vertically to have a bigger elliptical shape in the Diesel phase with the twofold of diameter. Also, it has been noted that the CNG bubbles velocity decreased as the magnetic field strengthened.

Keywords: Fuel technology; Liquid-gas fuel mixer; Magnetic field; Two phase hydro-magnetic flow.

NOMENCLATURE

A_b	bubble area
A_f	area of image frame
B	magnetic field intensity, Gauss
d_b	bubble diameter
D_i	pipe diameter
Gy_n	the y coordinate of the nth shape with area A_n
Gz_n	the z coordinate of the nth shape with area A_n
n	total number of bubbles
U_b	average bubble velocity
α	gas area fraction

1. INTRODUCTION

Carrying out the analysis about the flow dynamics of liquid and gas under the influence of both magnetic along with electric fields has turned into a significant factor in the control as well as design of several electric-apparatus systems such as magneto-hydrodynamic problems (MHD), gas and oil facilities, processing nuclear reactors and MHD power stations Ki (2010). The latest plan of pre-combining of CNG with Diesel was proposed in order to raise the amount of air in the cylinder to a greater extent, in the condition where a combination of air and CNG is added inside the engine, it can form a heavy mixture Abdul Wahhab *et al.* (2015). This mixture needs the investigation regarding the behavior of gas bubbles formed in the liquid fuels and the methods to manage their size prior to their arrival inside the injection system under the effect of external forces like magnetic field, in which the pattern of horizontal flow of bubbles is characterized by the presence of bubbles dispersed in a constant liquid phase, having a very small size than the diameter of the containing pipe. As compared to the vertical flow of the bubbles, the abovementioned flow direction has managed to get not as much of attention. Because of buoyancy, an additional difficulty arises in this case when the dispersed bubbles move to the top of the pipe and results in extremely non-symmetric volume fraction dispersion in the pipe cross-section Ekambara *et al.* (2008). Sussman and Smereka (1997) discussed that an example of complex flow simulation is the flow of two fluids with high density and viscosity ratios, such as bubbly along with droplets flow. They stated that the main concern is the behavior of gas bubble and its deformation in a viscous liquid. The mechanism of the movement of the bubbles and the

action of coalescence and bubble breakup is due to high density and viscosity ratios as well as topology changes. Hence, the inspection of the shape of the bubble domain in sporadic flows is very important to enhance the expectancy of the flow structure, flow pattern transition, as well as definition of a wide range of fluid properties. Bubble's shape along with velocities present in viscous liquids was deduced by Bhaga and Weber (1981) through conducting an experiment, whereas Brunner *et al.* (1980) and Brunner *et al.* (1983) suggested that the flow pattern may be controlled by electro-hydrodynamic forces and several flow pattern transition mechanisms were presented. So far, Ishimoto *et al.* (1995) carried out an experiment to study the effect on the bubbly flow because of non-uniform magnetic field, and made a comparison of the outcomes of the numerical as well as experimental outcomes carried out by Hnat and Buckmaster (1976), in which an outstanding acceptance was accomplished. On the other hand, many measuring techniques have been used to analyze the bubbly flow properties such as, ray absorption method, quick closing valve method, ultrasound method, electrical method, image processing techniques and magnetic resonance method Lugga (1999), Scheer (1996), Fossa (1998), Dinh and Choi (1999) techniques can be divided into intrusive and non-intrusive techniques according to whether flow fields are disturbed or not by the measuring equipment. Jarrahi *et al.* (2011) have used PIV technique to measure the velocity fields in the secondary flow and analyzed the variation in axial vorticity and transverse strain for different conditions that contributed to the mixing evaluation under different flow conditions.

Table 1 Properties of Diesel fuel and CNG

Parameter	Diesel Fuel	CNG
Density (kg/m^3)(20 ^{o}C)	840	0.72
Dynamic Viscosity (Pa.s) (20 ^{o}C)	2.49*10^{-3}	5.6*10^{-12}
LCV (Mj/kg)	43.8	45.8
Octane Number	50	125
Carbon (%, w/w)	86.83	73.3
Hydrogen (%, w/w)	12.72	23.9
Oxygen (%, w/w)	1.19	0.4
Sulphur (%, w/w)	0.25	ppm < 5
Electrical conductivity (pS/m)	250	-
Relative permittivity	2.0	-

Several studies have been carried out as shown in the literature review regarding effects of uniform magnetic fields on electric conductive vertical two-phase flows or non-uniform magnetic fields on two-phase flows. Though a complete study has not been found about the effects of variations in the intensity of a uniform magnetic field on the bubbly flow inside the horizontal pipes. Therefore, this study has been done on the effect caused due to the variation in the intensity of a uniform magnetic field on the bubbly flow of Diesel and CNG inside a horizontal pipe. CNG's bubbly flow behavior inside diesel exists in order to have an extensive variety of characteristics of two-phase flow (size and shape of bubbles, gas velocity, and gas area fraction). For this purpose, an analysis was executed over the bubbles of CNG inside laminar Diesel flow. Furthermore, this paper shows the outcomes of different magnetic field intensities on the CNG bubbly flow. All the experimental work was done by making the use of digital image processing technique. Properties of diesel fuel as well as CNG are shown in Table 1.

2. EXPERIMENTAL APPARATUS

A schematic diagram of the experimental facility for the concurrent two-phase (CNG-diesel) flow in a horizontal pipe is shown in Fig. 1(a). For the purpose of observation, the test portion of the facility was made up of transparent polycarbonate. The pipe was of length measuring 1.2 m and inner diameter (Di) of 0.02 m. The CNG bubbles generator had an induction system fitted on it, whose task was to produce liquid and gas mixture inside the test portion that was situated at the starting section of the test. The Diesel supply line and the compressed CNG line were linked to the bubble generator. Diesel flows by the bypass valve that is supplied and filtered by the fuel pump (90 watts, 5 l/min, 1.5 m) for the flow meter, pump along with the pressure gauge. After that, it goes into the side hole of the bubble generator and gets combined along with the CNG in order to a make two-phase flow. Then the compressed CNG goes into the mixer situated at the first edge of the bubble generator, via the center cross-sectional area. Use of a pressure regulator was made to control the pressure of CNG and flow rate of CNG was calculated by gas flow meter prior to its entrance in the bubble generator. One way valves were used for the purpose of controlling the CNG flow rate precisely. One needle of 0.1×10^{-3} m (inner diameter) was passed through the center of the cross-sectional area of pipe inside the bubble generator. Calibration of flow meter was done to record the flow rate of Diesel by making the use of a stopwatch. Moreover, the volume of the calibrated tank was pre-calibrated by height and its volume. The time consumed to fill 5 liters of diesel inside the tank was calculated. The time was approximately around 15 l/min; along with this, the accuracy was around ± 95%.

The electromagnet charger (excitation coils) was supplied by the DC power (Fig. 1b), it was made up of two coils having 250 wraps of copper wire that was covered by enamel having a diameter measuring 0.0021 m and a U-type yoke. The yoke was made with steel, the cross-sectional area for both of the yoke poles was 0.022 m that was perpendicular to the direction of the flow (X-axis) and 0.06 m that was parallel to the direction of flow (Z-axis) to embrace the test pipe in order to decrease the loss caused due to eddy current in the

core. A pair of the Tesla meter sensors was fixed between the yoke poles, and a test pipe was used to measure the magnetic intensity signing. The magnetic field between the excitation coils value designed in this work was measured having a variable magnetic field flux from 0 to 2000 Gauss.

Frame grabber board, high-speed camera, PC computer and a lighting system are the components of an image acquisition system. A 120 Watt lamp and a source of light, was kept at the back of the viewing pipe. The pictures were clicked using a Phantom Miro digital camera M 310 (maximum resolution: 1280*800). The frame rate of the camera was 3260 frames per second at 1280*800 and minimum exposure was 1.0 μsec. Use of the technique known as backlighting photography was utilized to record the shadow of CNG bubbles in bubbly flow as both diesel fuel and CNG bubbles were transparent. For the purpose of acquiring a smooth illumination of the section of the test, one layer of drawing sulfate paper was fixed at the back of the test section that resulted in an increase in the intensity of the contrast of the image and the silhouette of CNG bubbles.

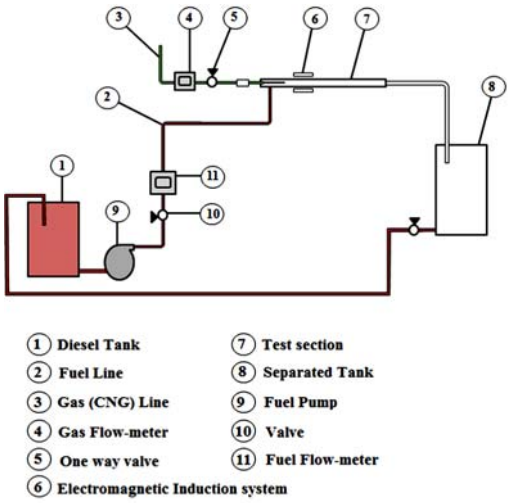

(a) The experimental rig

(b) Electromagnetic induction and Camera systems arrangement.

Fig. 1. The experimental rig and measurement system.

2.1 Uncertainty Analysis

The error analysis performed on the experimental data in order to evaluate the uncertainties in the measurements. The total uncertainty in every measurement can be obtained by combining the sensor accuracy and measuring instrument accuracy. A more realistic method is to use the root-sum-of-squares method, that is, by taking the square root of the sum of the individual errors Bevington and Robinson (2003).

$$\delta_{total} = \sqrt{(\delta_{sensor})^2 + (\delta_{instrument})^2} \quad (1)$$

Where, δ_{total} is the total uncertainty. The uncertainty percentage to the maximum and minimum values of recorded data was calculated from: Diesel flow meter, digital gas meter, and magnetic meter (Tesla-meter). Table 2 shows the uncertainty percentage error of the experimental yield values measured.

Table 2 the uncertainty percentage error of the experimental yield values measured

parameter	Min. for recorded value	Max. for recorded value	Min. and Max. uncertainty (%) error
Diesel flow rate	45.89 cm^3/s	90.75 cm^3/s	0.118 – 0.114
Gas flow rate	$9.714*10^{-4}$ cm^3/s	$1.119*10^{-2}$ cm^3/s	0.234 - 0.222
Magnetic field intensity	435 gauss	2000 gauss	0.132 – 0.122

3. DIGITAL IMAGE PROCESSING

The acquired images displayed that both the shape along with the size of the moving CNG bubbles are varying all the time under the influence of the magnetic field. The density variations, shape, gray level distribution, the size of the bubbles also had uneven variations from frame to frame. The edges of the CNG bubbles were not clearly observable particularly, which indicates that it is tough to get contour precisely through a simple detection method. Hence it is more appropriate for measuring and identifying the CNG-Diesel bubbly flow by making use of digital image processing. Image processing algorithm was developed to extract the information from the high-speed video data. The program was divided into three stages: bubble identification, verification of bubble parameters and bubble tracking. Fig. 2 shows a schematic of image processing used in the present work.

Each image was processed as a graphical object where each of the matrix contained three color intensities, the RGB values. The RGB image was converted into a grayscale image with 8 bit depth using rgb2gray function in Matlab. For gray level, all pixels consisted of a numerical value from 0 (black) to 255 (white). Images were cropped in order to retain only the part of the image immediately at the downstream of the nozzle, as shown in Fig. 3. After this cropping, the program recognizeed all frames when CNG bubbles started to release from the nozzle, thus providing the set of frames to be processed.

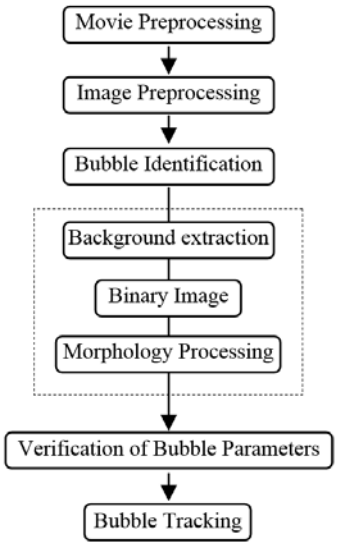

Fig. 2. Schematic of Image Processing Algorithm.

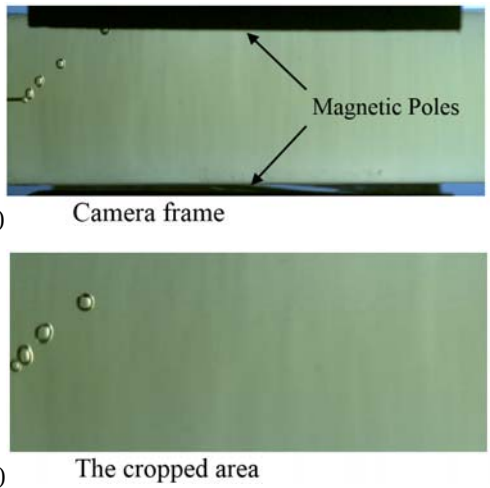

Fig. 3. The cropped area for Preprocessing of the images.

A number of preprocessing processes that should be performed in order to enhance the quality of the image as well as to decrease the noises are shown in Fig. 4. Previously image subtraction was utilized to lessen the background noise. Hence a calibration image was obtained with no bubbles. This image contained light distribution, information regarding the camera noise and background. The calibration image was subtracted from each image to provide an image of the bubble with reduced background noise. Moreover, each image was converted into a binary image by using a threshold of around 0.6-0.8. All pixels in the input image were replaced by output image having a larger luminance as compared to the threshold having a value 1 (white) as well as replacing all other pixels having value 0 (black), where it was possible to suppress light structures connected to the image. Thirdly, some morphological functions were used to improve the quality of the image and the bubble shape. Finally, images with the bubble were prepared for the next step that is the quantitative analysis which included evaluation of the center and size of the bubble. By counting the number of pixels in the bubble and scaling them to physical dimensions, the area of bubble was measured. By calibrating with the square mesh section (0.004*0.004 m) fixed in calibration pipe as shown in Fig. 5 (f), the area of the bubble could be determined. CNG bubbles in Diesel, the bubble shapes with changing magnetic intensity were estimated to spheres and oblate spheroids. The diameter of the bubble can be calculated as an equivalent diameter by assuming a round bubble shape:

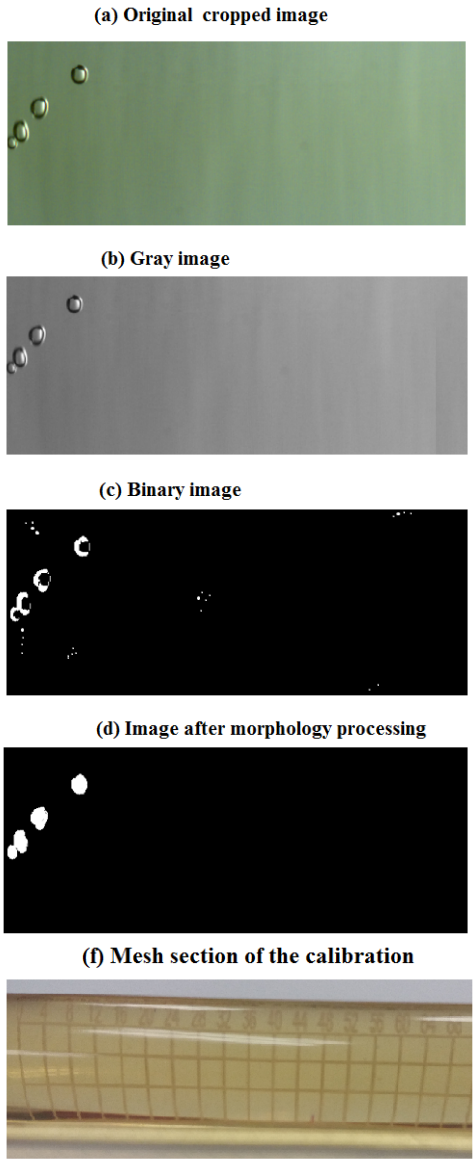

Fig. 4. Image processing procedures.

$$d_b = 2\sqrt{\frac{A_b}{\pi}} \tag{2}$$

The gas area fraction can be calculated by calculating the total area of all CNG bubbles in the image as shown below:

$$\alpha = A_f^{-1} \cdot \sum_{i=1}^{n} A_{bi} \tag{3}$$

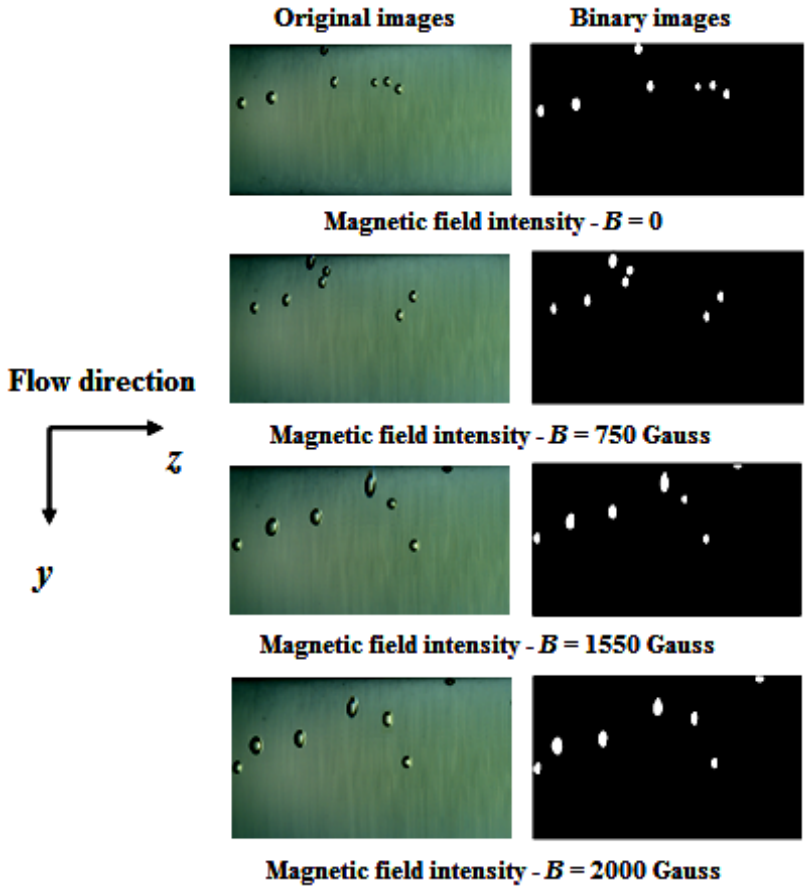

Fig. 5. Images and shape variations of CNG bubbles in Diesel flow with magnetic field intensity (0, 750, 1550, 2000 Gauss).

Where A_b is the bubble area, A_f stands for the area of the image frame, and n denotes the total number of bubbles in the image frame.

In Fig.4 (d), the top left coordinates are (0, 0), and the right bottom coordinates are (658, 239). The bubbles were numbered from top to bottom as well as from left to right. By using screen pixels and converting them into millimeter scale, sizes of CNG bubbles were measured. By counting the number of square pixels in each bubble, the area of bubble A_b, can be calculated. The next step was to track the CNG bubble from frame to frame in order, its trajectory and bubble velocity, this required bubbles' center. The geometric center of the bubble can be found as the center of mass of the region belonging to the bubble:

$$G_y = \frac{\sum_{i=1}^{n} A_n \cdot G_{y_n}}{\sum_{i=1}^{n} A_n} \tag{4}$$

$$G_z = \frac{\sum_{i=1}^{n} A_n \cdot G_{z_n}}{\sum_{i=1}^{n} A_n} \tag{5}$$

Where Gy_n is the y coordinate of the nth shape with area A_n, and Gz_n is the z coordinate of the nth shape with the area A_n. Once centroids for the first cropped image near the nozzle edge have been found, the algorithm moved the bubble border by a shift determined using the measured bubble velocity.

4. RESULTS AND DISCUSSION

4.1 The Effect of the Magnetic Field on CNG Bubble Sizes and Gas area Fraction

The experiment was carried out to investigate the effect on the growth of CNG bubbles of a magnetic field oriented normal to the flow. The results showed that CNG bubbles on the vertical magnetic field grow larger in the Diesel flow, increasing in the diameter at (750 Gauss, 1550 Gauss, and 2000 Gauss). Hence, the magnetic field caused by the Lorentz force to the adverse effect of the buoyance force devote to elongation in the bubbles and the mechanism to break off rather than pump driven. Fig. 5 shows images and shape variations of CNG bubbles in Diesel flow and the time increment is 0.1 sec, with magnetic flux of 0, 750, 1550 and 2000 Gauss. In this case, the CNG bubbles are changing from sphericity at injection time (t = 0) and nearly an oblate sphericity at the upper wall of test pipe. Moreover, this behavior is similar to

an increase in the magnetic field intensity, increase in bubble's size and gas area fraction. The experimental procedure was validated by comparing the current results with numerical results reported by Abdul Wahhab *et al.* (2016) and a good agreement was achieved. The bubbles size and gas area fraction with variation in magnetic field intensity are shown in Table 3.

Table 3 Measurements of CNG bubbles sizes and gas area fraction

$B = 0$			
Bubbles #	Area $\times 10^{-6}$ (m^2)	Diameter $\times 10^{-3}$ (m)	Center of bubbles (z, y)
1	0.984	1.12	(17.42, 104.25)
2	1.719	1.48	(58.76, 94.63)
3	0.753	0.98	(236.44, 6.98)
4	0.832	1.03	(264.71, 73.52)
5	0.453	0.76	(398.44, 69.62)
6	0.540	0.83	(422.73, 65.11)
7	0.678	0.93	(448.93, 78.67)
Gas area fraction		1.05 %	
$B = 750$ Gauss			
Bubbles #	Area $\times 10^{-6}$ (m^2)	Diameter $\times 10^{-3}$ (m)	Center of bubbles (z, y)
1	0.751	0.98	(38.14, 98.41)
2	0.849	1.04	(78.74, 71.41)
3	1.86	1.54	(211.66, 9.48)
4	0.738	0.97	(239.46, 33.42)
5	1.002	1.13	(246.74, 23.76)
6	0.832	1.03	(453.76, 102.31)
7	0.932	1.07	(472.12, 62.12)
Gas area fraction		1.23 %	
$B = 1550$ Gauss			
Bubbles #	Area $\times 10^{-6}$ (m^2)	Diameter $\times 10^{-3}$ (m)	Center of bubbles (z, y)
1	0.882	1.06	(9.71, 138.41)
2	2.6	1.82	(63.48, 111.32)
3	2.034	1.61	(232.44, 86.43)
4	3.015	1.96	(353.52, 28.43)
5	0.678	0.93	(434.22, 61.76)
6	0.751	0.98	(486.74, 143.21)
7	0.301	0.62	(521.42, 5.34)
Gas area fraction		1.812 %	
$B = 2000$ Gauss			
Bubbles #	Area $\times 10^{-6}$ (m^2)	Diameter $\times 10^{-3}$ (m)	Center of bubbles (z, y)
1	0.849	1.04	(7.32, 148.11)
2	2.349	1.73	(40.33, 124.14)
3	2.111	1.64	(209.41, 101.32)
4	2.715	1.86	(321.66, 51.84)
5	1.627	1.44	(429.31, 66.39)
6	0.832	1.03	(461.44, 139.74)
7	0.607	0.88	(531.42, 5.94)
Gas area fraction		1.959 %	

4.2 The Effect of Magnetic Field on the CNG Bubble Velocity

Figure 6 shows the translational average velocity of the bubbles (U_b) during 1.0 sec time, at various magnetic field intensities. The general trend of the velocity of CNG bubble decreased as the magnetic field strength increased. The figure presents the time development of the CNG bubble velocity for changing magnetic field intensity (0, 750, 1550, and 2000 gauss). It can be observed in Fig. 6 that increasing magnetic field intensity decreases the average CNG bubble velocity. The effect of the magnetic field normal to the flow direction results in a drag-like or resistive force bearing the tendency to suppress the movement of the liquid in the pipe to make it slow, which, in turn, decreases the motion of the gas bubble. This is translated into the reductions in the average velocity of bubbles (CNG) phase and their flow rate. Moreover, the reduced motion of the CNG bubbles in the pipe that occurs by increasing the strength of the magnetic field results in lower velocity gradients at the wall. This has a direct effect in increasing the period of transfer of momentum of both of phases.

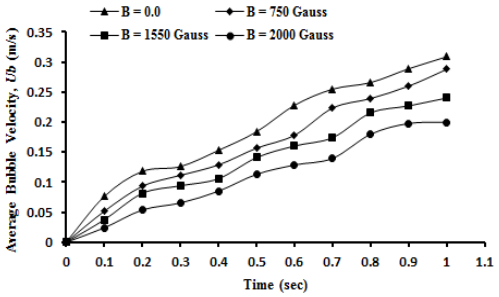

Fig. 6. The average bubble velocity at various magnetic field intensity(0, 750, 1550, and 2000 Gauss).

5. CONCLUSION

This work conducts a visualization of the CNG bubbles inside the laminar diesel flow in a horizontal pipe under the influence of different magnetic field strengths. In order to carry out the analysis of the experimental data, digital image processing technique was implemented. The following conclusions could be drawn from the analysis of the results:

- CNG bubbles change from sphericity at injection time (t = 0) and nearly an oblate sphericity at the upper wall of test pipe. Furthermore, this behavior is similar when magnetic field intensity and the bubble size is increased.
- CNG bubbles tend to move towards the upper wall under buoyancy effect and these bubbles develop into a bigger size and expand in the diesel flow field.
- By increasing magnetic field intensity, gas area fraction value increases.

- By increasing the magnetic field strength, the average bubble velocity decreases.

It is highly recommended to visualize the CNG bubbles in the laminar Diesel flow in a horizontal pipe under the effect of various magnetic field strengths of higher ranges that were utilized in this work.

ACKNOWLEDGEMENTS

The authors are grateful to the University Technology PETRONAS for providing the center for automotive research and energy management (CAREM).

REFERENCES

Abdul Wahhab, H. A., A. R. A. Aziz, H. H. Al Kayiem and M. S. Nasif (2016). Modeling of mixing Diesel-CNG in a horizontal pipe under the influence of a magnetic field, *Asian Journal of Applied Sciences.* 4(4), 920-929.

Abdul Wahhab, H. A., A. R. A. Aziz, H. H. Al Kayiem and M. S. Nasif (2015). Modeling of diesel/CNG mixing in a pre-injection chamber. *3rd International Conference Mechanic Engineering Research, IOP Conference Series*. 100, 012044.

Bevington, P. R. and D. Keith Robinson (2003). Data reduction and error analysis. McGraw-Hill.

Bhaga, D. and M. E. Weber (1981). Bubbles in viscous liquids: shapes, wakes and velocities, *Journal of fluid Mechanics* 105, 61-85.

Brunner, K. and J. S. Chang (1980). Flow regime transition under electric fields in horizontal two-phase flow. in proceedings, *15th IEEE Industry Applications Society Conference* 1052-1058.

Brunner, K., P. T. Wan and J. S. Chang (1983). Flow pattern maps for horizontal gas liquid two-phase flow under d.c. electric field. *In Electrostatics, Institute of Physics Conference Series 66*, 215-220.

Dinh, T. B. and T. S. Choi (1999). Application of image processing techniques in air/ water two phase flow, *Mechanics Research Communications* 26(4), 463-468.

Ekambara, K., R. S. Sanders, K. Nandakumar and J. H. Masliyah (2008). CFD simulation of bubbly two-phase flow in horizontal pipes, *Chemical Engineering Journal*. 144, 277–288.

Fossa, M. (1998). Design and performance of a conductance probe for measuring the liquid fraction in two-phase gas-liquid flows. *Flow Measurement and Instrumentation* 9, 103-109.

Hnat, J. G. and J. D. Buckmaster (1976). Spherical cap bubbles and skirt formation. *The Physics of Fluids* 19, 182-194.

Ishimoto, J., M. Okubo, S. Kamiyama and M. Higashitani (1995). Bubble behavior in magnetic fluid under a non-uniform magnetic field, *International Journal of JSME* 38(3), 382-387.

Jarrahi, M., C. Castelain and H. Peerhossaini (2011). Laminar sinusoidal and pulsatile flows in a curved pipe, *Journal of Applied Fluid Mechanics* 4(2), 21- 26.

Ki, H. (2010). Level set method for two-phase flows under magnetic fields, *Computer Physics Communications* 999-1007.

Lugga, R. D. (1999). Energy dispersive X-ray scatter for measurement of oil/water ratios, *Unclear Instruments and Methods in Physical Research* 422, 938-941.

Scheer, A. M. (1996). Multiphase Flow Measurement Using Multiply Energy Gamma Ray Absorption (MFGRA) Composition Measurement. *SPE 36593 Presented at 1996 Annual-Technical Conference and Exhibition, Denver Colorado* 10, 6-9.

Sussman, M. and J. A. Smereka (1997). Axisymmetric free boundary problems. *Journal of Fluid Mechanics* 341, 269-294.